Proc. CIBSE A: Building Serv. Eng. Res. Technol. 18(2) 67–75 (1997) Printed in Great Britain B413

Summary This paper presents a methodology for predicting air flow and thermal comfort in naturally ventilated buildings. Numerical simulations were carried out for a naturally ventilated room with heat-pipe heat recovery. The RNG k–ϵ turbulence model was used for simulations. Calculation of air flow rates in the room took into account not only of driving forces (wind and stack effects) but also flow resistances (pressure loss due to heat pipes and other duct fittings and friction loss in air ducts). The potential of a heat-pipe heat recovery system to produce adequate thermal comfort in naturally ventilated buildings is investigated using CFD. The importance of proper control of air flow rate is highlighted.

Naturally ventilated buildings with heat recovery: CFD simulation of thermal environment

G Gan BSc PhD and **S B Riffat** MSc PhD CEng MIMechE MCIBSE MInstE
Institute of Building Technology, Department of Architecture and Building Technology, University of Nottingham, Nottingham NG7 2RD, UK

Received 13 August 1996, in final form 10 October 1996

List of symbols

A Opening area (m^2)
C Mean concentration of water vapour in air (kg kg^{-1})
C_d Discharge coefficient
C_p Pressure coefficient
C_{pa} Specific heat capacity of dry air (J $kg^{-1}K^{-1}$)
C_{pv} Specific heat capacity of water vapour (J $kg^{-1}K^{-1}$)
C_s Volumetric moisture production rate (kg $s^{-1}m^{-3}$)
g Acceleration due to gravity (m s^{-2})
H Mean enthalpy of air mixture (J kg^{-1})
h Stack height (m)
h_{fg} Latent heat of evaporation (J kg^{-1})
K Velocity pressure loss coefficient of duct fitting
K_f Friction loss coefficient of straight duct
K_i Pressure loss coefficient per unit length along direction i (m^{-1})
k Turbulent kinetic energy (kg m^2s^{-2})
P_v Velocity pressure based on duct mean velocity (Pa)
P_{vw} Wind velocity pressure at roof level (Pa)
PD Percentage of dissatisfied due to draught (%)
PMV Predicted mean vote
PPD Predicted percentage of dissatisfied (%)
p Local static pressure (Pa)
ΔP Pressure difference between supply and exhaust openings (Pa)
ΔP_b Pressure difference due to stack effect (Pa)
ΔP_f Friction loss in straight duct (Pa)
ΔP_h Pressure loss due to duct fitting (Pa)
ΔP_w Pressure difference due to wind effect (Pa)
Q Air flow rate (m^3s^{-1})
q Volumetric heat production/dissipation rate (W m^{-3})
T Mean air temperature (°C)
T_r Mean radiant temperature (°C)
T_{res} Dry resultant temperature (°C)
U_i Mean velocity component in direction i (m s^{-1})
V Resultant mean velocity (m s^{-1})
V_w Wind speed at roof level (m s^{-1})
x_i Co–ordinate in tensor notation
z Height above ground (m)
α Inverse Prandtl number
δ_{ij} Kronecker delta ($\delta_{ij} = 1$ if $i = j$ and $\delta_{ij} = 0$ if $i \neq j$)
ε Turbulent dissipation rate (m^2s^{-3})
μ Laminar viscosity (kg $m^{-1}s^{-1}$)
μ_e Effective viscosity (kg $m^{-1}s^{-1}$)
μ_t Turbulent viscosity (kg $m^{-1}s^{-1}$)
ρ Air density (kg m^{-3})

1 Introduction

Natural ventilation has many environmental advantages. It is being exploited as an alternative to mechanical ventilation and air conditioning in large or commercial buildings. However, few designers have considered heat recovery from naturally ventilated buildings. This may be partly due to the pressure losses arising from two separate sources. The first is the direct pressure loss caused by a conventional heat recovery system, resulting in insufficient air exchange. The second is the indirect pressure loss resulting from the reduced temperature difference between supply and exhaust when heat is recovered from return air. These losses can be reduced by taking appropriate measures. For example, the stack effect can be increased using a higher stack or by employing solar energy. The pressure loss through a heat recovery system can also be reduced using heat pipes instead of conventional heat exchangers.

A heat-pipe heat recovery unit is a heat exchanger consisting of externally finned sealed pipes using a working fluid such as methanol. The unit is divided into two sections, evaporator and condenser, for heat exchange between return and supply air (see Figure 1). A divider prevents the two air streams mixing. Warmer return air in the exhaust duct is passed over one end of the heat pipe (evaporator section) and so evaporates the refrigerant in the pipe. The less dense refrigerant vapour travels to the opposite end of the heat pipe (condenser section), leading to transfer of heat from the evaporator section to the condenser section. When cooler outdoor air is passed over this end of the heat pipe, the refrigerant vapour condenses. The condensed liquid returns to the heat pipe evaporator by gravity or capillary effects, providing a continuous heat exchange process.

A heat-pipe heat exchanger has a number of advantages over conventional heat exchangers[1]. They include:

(*a*) no moving parts, no external power requirements and so high reliability

(*b*) no cross–contamination because of a solid wall between the warm and cold air streams

(*c*) compact and suitable for all temperature applications in heating, ventilation and air–conditioning (hvac)

(*d*) fully reversible, i.e. heat transferable in either direction

(*e*) easy cleaning.

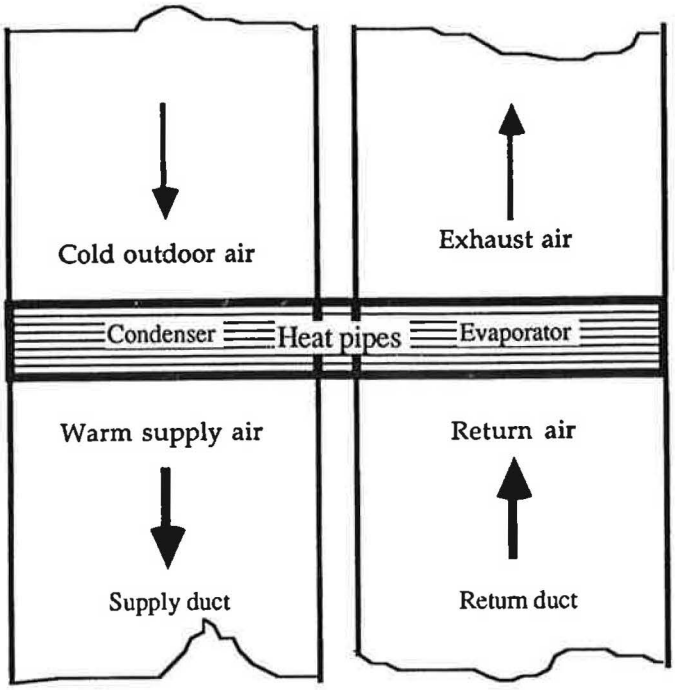

Figure 1 Schematic representation of the heat-pipe heat recovery unit in operation

Since evaporation/condensation cycle effects of heat pipes are reversible, they are used not only to recover heat from return air but also to precool supply air by rejecting heat to a cold exhaust duct. Heat pipes are becoming more commonly used in the air-conditioning industry, although this is at present mainly confined to applications where humidity must be controlled. Supermarket air conditioners are an example. Hill and Lau[2] conducted six field studies of supermarket air conditioning systems equipped with heat-pipe heat exchangers operating in various climates. Substantial savings in refrigeration energy were achievable with a reduction of indoor humidity. The performance of a heat-pipe heat exchanger (HPHX) for air conditioning applications was also evaluated through a combination of a detailed HPHX thermal node model and a model for the air-conditioning system[3]. It was suggested that the use of an HPHX could offer significant improvements in moisture control and overall efficiency compared with the conventional practice of using a specially designed cooling coil in combination with reheat.

Over recent years computational fluid dynamics (CFD) has increasingly been applied to simulations of room air movement, temperature and other comfort-related parameters in order to optimise thermal design of buildings and associated hvac systems. Most computations are based on the standard k–ε turbulence model developed by Launder and Spalding[4]. Chen[5] compared five different k–ε models including the standard, renormalisation group (RNG) and low-Reynolds-number models for indoor air flow computations. It was found that the standard and RNG k–ε models were very stable compared with the low-Re k–ε model. The latter also had the disadvantage of requiring a very fine grid distribution in the near-wall region and hence a significantly higher computing cost. Comparison of the standard and RNG k–ε models showed that the RNG k–ε model was slightly superior and this was therefore recommended for indoor air flow computations[5].

The objective of the present study is to assess the performance of heat pipes in naturally ventilated buildings. This will be carried out through comparison of the predicted indoor thermal environment with and without heat-pipe heat recovery using CFD with the RNG k–ε turbulence model.

2 Air flow rate

CFD simulation of the indoor environment of a naturally ventilated room requires the calculation of air flow rate.

The air flow rate through openings of a naturally ventilated room with heat-pipe heat recovery depends on the wind and stack effects and on pressure losses through the heat-pipe unit and air duct. For the ventilation system illustrated in Figure 2, the flow rate can be calculated using the following equation[6]:

$$Q = C_d A(2\Delta P/\rho)^{1/2} \quad (1)$$

where Q is the flow rate (m^3s^{-1})m, C_d is the discharge coefficient; A is the effective opening area (m^2), ΔP is the net pressure difference between the supply and exhaust openings (Pa) and ρ is the air density (kg m^{-3}).

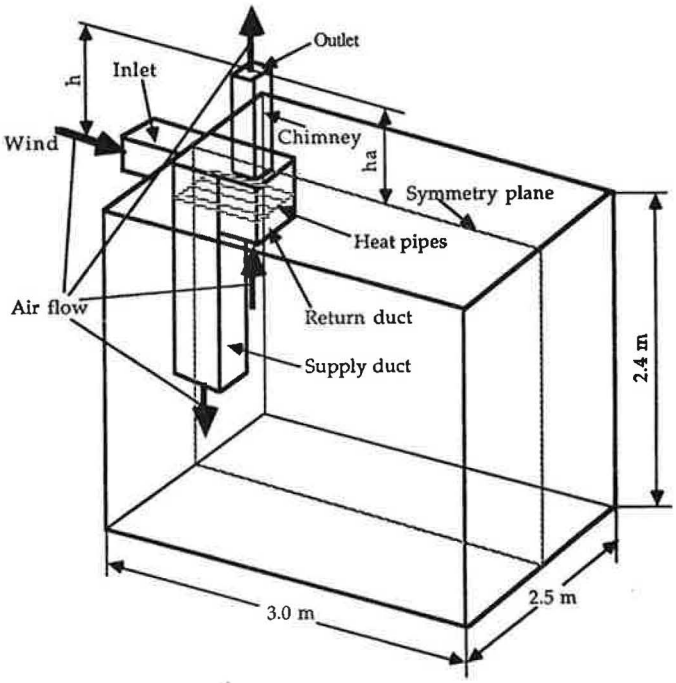

Figure 2 Schematic diagram of the naturally–ventilated room with heat pipe heat recovery unit

The effective area for two openings in series is given by:

$$1/A^2 = 1/A_s^2 + 1/A_e^2 \quad (2)$$

where A_s and A_e are the areas of supply and exhaust openings, respectively (m^2).

The density for a mixture of dry air and water vapour is given by[7]:

$$\rho = 353.06/(T + 273.15)(0.61C + 1) \quad (3)$$

where T is the mean air temperature (°C) and C is the mean concentration of water vapour in air (kg kg^{-1}). The density may be considered approximately to be a function of air temperature only. This could, however, result in errors of 2% in density difference for calculating the buoyancy effect under winter conditions and 8% in summer conditions[8].

The net pressure difference is the difference between driving pressures and flow resistances. The driving pressures due to

natural forces are the wind pressure difference ΔP_w and the stack pressure difference ΔP_b. The flow resistances include friction loss in straight ducts ΔP_f and pressure loss through duct fittings such as heat pipes and bends ΔP_h Therefore

$$\Delta P = \Delta P_w + \Delta P_b - \Sigma\Delta P_f - \Sigma\Delta P_h \quad (4)$$

where

$$\Delta P_w = (C_{ps} - C_{pe}) P_{vw} \quad (5)$$

$$\Delta P_b = (\rho_s - \rho_e) g h \quad (6)$$

$$\Delta P_f = K_f P_v \quad (7)$$

$$\Delta P_h = K P_v \quad (8)$$

C_p is the pressure coefficient, subscripts s and e denote the values associated with supply and exhaust openings, P_{vw} (= $^1/_2\rho V_w^2$) is the wind velocity pressure at roof level (Pa), V_w is the wind speed at roof level (m s^{-1}); g is the acceleration due to gravity (m s^{-2}), h is the stack height (m); P_v is the velocity pressure based on the duct mean velocity (Pa), and K and K_f are the velocity pressure loss coefficient of duct fittings including the heat pipe unit and the friction loss coefficient of the straight duct respectively (dimensionless).

The wind speed at roof level in an urban terrain is given by[6]:

$$V_w = 0.35\, V_{10} z^{0.25} \quad (9)$$

where V_{10} is the mean wind speed at 10 m height (m s^{-1}) and z is the height above ground (m).

The velocity pressure loss coefficient K can be determined experimentally or, for fittings such as perforated plates and bends, can be predicted using CFD modelling[9,10]. The friction pressure loss in a short straight duct is small compared with the pressure loss through a perforated plate used in practice. Consider for example air flowing through a perforated plate of 50% free area in a 1 m length of 0.2 m diameter galvanised sheet steel duct at a velocity of 10 m s^{-1}. The friction loss is only 3% of the pressure loss across the plate (K_f/K = 0.105/3.5 = 0.03)[10].

3 Modelling of heat pipes

The heat-pipe heat recovery unit is modelled as a porous medium with heat generation (for condenser section) and dissipation (for evaporator section). A porous media model is used to predict air flow and pressure loss through the unit and heat transfer between the unit and air.

The porous media model incorporates a flow resistance in a region occupied by the porous medium. The model is a sink in the standard momentum equations (described in the next section) for the porous medium and is represented by the following equation in Cartesian tensor notation:

$$\partial p_h/\partial x_i = K_i(^1/_2\rho U_i|U_i|) \quad (10)$$

where $\partial p_h/\partial x_i$ is the pressure gradient in the porous medium in direction i (Pa m^{-1}), K_i is the pressure loss coefficient per unit length along direction i (m^{-1}) and U_i is the mean velocity component in direction i (m s^{-1}).

4 Air flow model

The air flow model consists of a set of governing equations representing continuity, momentum, turbulence, enthalpy and concentration. In this study, the RNG k–ε turbulence model developed by Yakhot and Orszag[11] and Yakhot *et al.*[12] is used. For an incompressible steady-state flow the time-averaged equations are as follows:

Continuity:

$$(\partial/\partial x_i)(\rho U_i) = 0 \quad (11)$$

Momentum:

$$(\partial/\partial x_j)(\rho U_i U_j) = (\partial/\partial x_j)[\mu_e (\partial U_i/\partial x_j + \partial U_j/\partial x_i)] - (\partial/\partial x_j)(p - p_h + {}^2/_3\rho k\delta_{ij}) + g_i(\rho_r - \rho) \quad (12)$$

where p is the local static pressure (Pa), δ_{ij} is the Kronecker delta (δ_{ij} = 1 if $i = j$ and δ_{ij} = 0 if $i \neq j$), μ_e is the effective viscosity (kg m^{-1}s^{-1}), g_i is the component of gravitational acceleration in direction i (m s^{-2}), ρ_r is the air density at a reference point (kg m^{-3}) and k is the turbulent kinetic energy (m^{2}s^{-2}).

The effective viscosity is the sum of turbulent (μ_t) and laminar (μ) viscosities, i.e. $\mu_e = \mu_t + \mu$. The turbulent viscosity is:

$$\mu_t = \rho C_\mu k^2/\varepsilon \quad (13)$$

where C_μ = 0.085 and ε is the turbulent dissipation rate (m^{2}s^{-3}).

Turbulent kinetic energy:

$$(\partial/\partial x_i)(\rho U_i k) = (\partial/\partial x_i)(\alpha_k \mu_e \partial k/\partial x_i) + \mu_t S^2 - \rho\varepsilon + (g_i/\rho)\alpha_t \mu_t \partial\rho/\partial x_i \quad (14)$$

Turbulent dissipation rate:

$$(\partial/\partial x_i)(\rho U_i \varepsilon) = (\partial/\partial x_i)(\alpha_e \mu_e \partial\varepsilon/\partial x_i) + C_1\mu_t S^2\varepsilon/k - C_2\rho\varepsilon/k + C_3 (g_i/\rho)\alpha_t\mu_t\partial\rho/\partial x_i\,(\varepsilon/k) - \rho R \quad (15)$$

In equations 14 and 15, C_1 = 1.42, C_2 = 1.68, C_3 = tanh(V_g/V_h) with V_g and V_h the mean velocity components in vertical and horizontal directions respectively; α_k, α_e and α_t are the inverse Prandtl numbers for turbulent transport and R is the rate of strain.

α_k, α_e and α_t are computed via:

$$\frac{|(\alpha - 1.3929)/(\alpha_0 - 1.3929)|^{0.6321}}{|(\alpha + 2.3929)/(\alpha_0 + 2.3929)|^{0.3679}} = \mu/\mu_e \quad (16)$$

$\alpha_k = \alpha_e = \alpha$ with α_0 = 1.0 and $\alpha_t = \alpha$ with α_0 the laminar inverse Prandtl number.

R is given by

$$R = C_\mu \eta^3 (1 - \eta/\eta_0)/(1 + \beta\eta^3)(\varepsilon^2/k) \quad (17)$$

where

$$\eta_0 = 4.38 \qquad \beta = 0.012 \qquad \eta = Sk/\varepsilon$$

$$S = (2S_{ij}S_{ij})^{1/2} \qquad S_{ij} = {}^1/_2(\partial U_i/\partial x_j + \partial U_j/\partial x_i)$$

Enthalpy:

$$(\partial/\partial x_i)(\rho U_i H) = (\partial/\partial x_i)(\alpha_t \mu_e \partial H/\partial x_i) + q \quad (18)$$

where H is the mean enthalpy of air mixture (J kg^{-1}) and q is the volumetric heat production/dissipation rate (W m^{-3}).

Concentration:

$$(\partial/\partial x_i)(\rho U_i C) = (\partial/\partial x_i)(\alpha_t \mu_e \partial C/\partial x_i) + C_s \quad (19)$$

where C_s is the volumetric moisture production rate (kg s^{-1}m^{-3}).

Air temperature is calculated from the enthalpy of air mixture and concentration of water vapour via

$$H = (C_{pa} + C_{pv}C)T + h_{fg}C \quad (20)$$

where C_{pa} and C_{pv} are the specific heat capacities of dry air and water vapour respectively (J kg^{-1}K^{-1}) and h_{fg} is the latent heat of evaporation (J kg^{-1}).

The boundary conditions for solving the flow equations are described by Gan[7]. The governing equations are solved for the three–dimensional Cartesian system using the SIMPLE algorithm and the power law differencing scheme[13].

The overall structure of the computer program follows a two–dimensional TEAM computer code[14]. The original 2D code is extended to 3D conditions and modified for simulations of air, heat and moisture movement in buildings.

The supply air flow rate depends on the exhaust air temperature and pressure loss through the ventilation system, which are in turn dependent on indoor air flow patterns as well as heat generation and distribution. The supply air flow rate is therefore obtained through iteration in the solution of air flow equations.

The solution was considered to have converged when the sum of the normalised residuals was less than 10^{-6} for enthalpy and less than 10^{-3} for other flow equations. Convergence was achieved after 5000 to 11 000 iterations, depending on the ventilation system arrangement and rate of heat production in the room. The slow convergence was caused by the interdependence between the air flow rate, flow pattern and air temperature distributions. For a grid size of 44 × 36 × 21 for room length, height and half width, the CPU time for the calculation of the equations was about 36 seconds per iteration on a 6–processor Sun SPARCserver 1000E.

5 Thermal comfort

Thermal comfort can be assessed using indices such as resultant temperature, thermal sensation and draught risk.

The resultant temperature is given by[6]

$$T_{res} = [T_r + T(10V)^{1/2}]/[1 + (10V)^{1/2}] \quad (21)$$

where T_{res} is the dry resultant temperature (°C), V is the mean air velocity (m s^{-1}) and T_r is the mean radiant temperature (°C) which can be calculated from the temperature and other characteristics of room surfaces[7].

Thermal sensation is assessed in terms of predicted mean vote (PMV) and predicted percentage of dissatisfied (PPD). These indices depend on air velocity, temperature, humidity and mean radiant temperature together with personal factors such as clothing and activity. Details of the derivation are given by Fanger[15]. The assessment of thermal sensation is particularly important for rooms with substantial surface temperature variations[7].

Draughts in naturally ventilated buildings are usually not as serious as in air–conditioned buildings, but can still cause discomfort along cold air streams. The risk of draught is calculated for isotropic turbulence on the basis of the draught model by Fanger *et al.*[16]:

$$PD = (3.143 + 52.56k^{1/2})(34 - T)(V - 0.05)^{0.6223} \text{ for } V > 0.05 \text{ m s}^{-1}$$
$$PD = 0.0 \text{ for } V \leq 0.05 \text{ m s}^{-1} \quad (22)$$

where PD is the percentage of dissatisfied due to draught (%).

6 Results and discussion

Simulations were performed for a test chamber as a naturally ventilated room in the heating period as shown in Figure 2. The room is 3.0 m long, 2.5 m wide and 2.4 m in ceiling height. It is assumed that all the room walls are insulated. The cross–sectional area of air supply and exhaust openings is 0.01 m^2. The duct cross–section is 0.2 m square. The room and ventilation system are symmetrical along the plane of the mid–width and so only half of the room is used for simulations. The simulated room has a uniformly distributed heat source on the floor totalling 200 W. It is assumed that half of the heat is reclaimed by the heat recovery unit. Heat is generated on the condenser section of the heat recovery unit at 100 W and the same amount dissipates on the evaporator section. The outdoor air is set at 5 °C and 90% relative humidity. The chimney height is 1 m above the roof level. The wind speed V_{10} is assumed to be 3 m s^{-1} and the wind direction is perpendicular to the wall with the supply opening.

Seven simulations were performed for different supply air conditions or heat production rates. The results are presented in Table 1.

Figure 3 shows the predicted air movement, air temperature, humidity and thermal comfort indices on the symmetrical plane in the room with heat-pipe heat recovery (No. I). As seen from the figure, the incoming air flows along the supply duct and then spreads over the floor. However, the room air is stagnant (mean air velocity < 0.1 m s^{-1}) except for areas in the supply air stream and near the wall surfaces. The predicted air flow rate is 6.9 l s^{-1}, i.e. 1.4 air changes per hour.

From the prediction, the supply air is heated from an outdoor air temperature of 5 °C to 10 °C when passing the heat pipes. Along the supply air stream, the air temperature is low (< 19 °C). Apart from this area, the room temperature is relatively uniform with a mean air temperature in the occupied zone (air space from floor to 1.8 m high and 0.15 m away from side walls) of 19.3 °C. The vertical air temperature difference between 1.1 m and 0.1 m above the floor is 2.2 K, lower than the comfort limit of 3 K[17].

The predicted relative humidity in the occupied zone is 35.2%. This is below the lower comfort limit (40%) recommended by CIBSE[6]. The simulation is, however, carried out for the empty room. Under realistic conditions, the room humidity will be increased as a result of moisture production by occupants. For example, suppose the room were occupied by an office worker with a latent heat emission of 40 W[6]. The moisture production calculated from the latent heat is 16 5 10^{-3} g s^{-1}. Assuming the moisture was uniformly distributed in the room, it would be equivalent to an increment in the moisture content of air of about 1.9 g kg^{-1} at the predicted flow rate. This could have raised the relative humidity from 35% to approximately 46% at 19.3 °C.

The average room surface temperature is 21.1 °C, higher than the air temperature. As a result, the mean radiant temperature and resultant temperature in the room are higher than the air temperature. The calculated resultant temperature for the occupied zone is 20 °C. Also, the distribution of resultant temperature (Figure 3(d)) is more uniform than that of air temperature (Figure 3(b)). This is due to the higher floor temperature than temperatures of other room surfaces, resulting in a high radiant temperature near the floor which partly compensates for the low air temperature. Thus the room is on average, comfortable according to CIBSE[6].

Table 1 Predicted room thermal environment

Parameter	Prediction number						
	I	II	III	IV	V	VI	VII
Heat pipes installed?	Yes	No	No	No	Yes	No	Yes
Wind effect included?	Yes	Yes	Yes	Yes	No	No	No
Air flow rate (l s^{-1})	6.9	7.6	7.4	7.8	4.1	4.6	8.5
Outdoor air temp. (°C)	5.0	5.0	5.0	5.0	5.0	5.0	5.0
Supply air temp. (°C)	10.0	5.0	10.0	5.0	11.9	5.0	9.1
Exhaust air temp. (°C)	5.4	16.1	19.2	18.0	20.0	19.7	13.8
Heat from floor (W)	200	200	200	300	200	200	200
Air velocity† (m s^{-1})	<0.1	<0.1	<0.1	<0.1	<0.1	<0.1	<0.1
Air temp.† (°C)	19.3	15.3	18.9	17.5	27.2	19.1	19.0
Relative humidity† (%)	35.2	45.3	36.1	39.4	21.8	35.6	35.7
Mean radiant temp (°C)	20.7	16.7	20.4	19.8	28.5	19.1	20.5
Resultant temp.† (°C)	20.0	16.0	19.6	18.6	27.9	19.1	19.8
Predicted mean vote	–0.4	–1.2	–0.5	–0.7	1.2	–0.6	–0.5
Predicted percentage of dissatisfied (%)	8.9	37.4	10.5	15.8	36.7	12.6	9.8
Draught risk† (%)	1.6	1.9	1.5	2.0	0.7	1.0	1.5
Temp gradient‡ (K)	2.2	2.6	2.0	2.5	2.1	2.2	2.0
Floor temp. (°C)	28.7	24.3	28.5	32.2	36.6	28.2	28.7
Ceiling temp. (°C)	19.8	16.1	19.1	17.9	27.6	19.4	19.4
Mean wall temp. (°C)	21.1	16.8	21.3	19.9	28.4	20.5	20.5

† Average for the occupied zone

‡ Vertical air temperature difference from 1.1 m to 0.1 m above the floor

The prediction of thermal sensation is based on the metabolic rate of 1.2 met (70 W m^{-2} of skin area) and clothing level of 1.0 clo (= 0.155 $m^2K\ W^{-1}$) for an imaginary sedentary occupant in winter conditions. The predicted thermal sensation for the occupied zone is within the comfort limit (–0.5 < PMV < 0.5 and PPD < 10%[17]). However, due to the low air temperature, the air near the floor is slightly cool (PMV < –0.5) (Figure 3(e)).

The draught risk in the room is small because of low velocities (Figure 3(f)), although just below the supply outlet it is above the comfort limit of 15%[16].

When the heat recovery unit is removed from the ventilation system (No. II), the predicted air temperature in the room is much lower than the comfort requirement with a mean value of 15.3°C (Figure 4(b)). As a result, however, the relative humidity is increased to an acceptable level (Figure 4(c)). The average air temperature difference from 1.1 m to 0.1 m above the floor is still within the comfort limit. However there may be a local discomfort near the supply outlet where the vertical temperature gradient is higher than 3 K. The predicted air flow rate through the room is slightly (10%) higher than that with heat recovery, due to a small increase in the temperature difference between exhaust and supply air and to the absence of the flow resistance of the heat recovery unit. Because of the low air temperature, the room is cool with the resultant temperature below 16°C (Figure 4(d)) and below PMV –1.2 (Figure 4(e)). Besides, the draught risk above 15% extends to half of the room length near the floor (Figure 4(f)).

Without the heat recovery unit but with the supply air temperature heated to 10°C (No. III), which would be the same as passing the air over heat pipes, the predicted air temperature is similar to that predicted with the heat recovery unit (Figure 5). This indicates that the heat recovery unit performs well as an air heater.

With the same supply air conditions as for No. II but the heat production from the floor increased to 300 W (No. IV), the predicted room air temperature is on average 1°C lower than the temperature with supply air heated using the same amount of heat (Figure 6). Besides, the predicted temperatures of room surfaces differ substantially with floor heating; the temperature difference between floor and ceiling is 14.3 K. As a result, although the floor temperature with floor heating is higher, and already over the comfort limit of 29°C[17], the average room surface temperature is still lower than that with air heating. The room is slightly cool with less PMV than –0.5. This shows that for this room it is better to provide heat for the supply air than to heat the floor excessively using an underfloor system.

When the air flow due to the wind effect is neglected (No. V), for the same ventilation opening size and heat recovery unit as No. I, the predicted flow rate is reduced by 41% to 4.1 l s^{-1}; this is much lower than the minimum fresh air requirement for one occupant[6]. The predicted room temperature is increased to 27.2°C, too high for thermal comfort at low velocities (Figure 7). The room thermal environment is warm, as the predicted value for PPD is 36.7% and greater than 1.2. When the heat recovery unit is removed (No. VI), the average room air temperature is reduced to an acceptable level for thermal comfort but the air temperature near the floor is low (Figure 8). Consequently, the room is slightly cool (= –0.6). Besides, there is likely a local discomfort due to vertical temperature gradient (> 3 K).

For the same heat recovery unit but with the size of inlet and outlet openings increased to the same size as the air duct (0.2 × 0.2 m) (No. VII), the predicted air flow rate is more than doubled as compared with No. V. The room air temperature is 19°C and the PPD is less than 10%. Hence this ventilation arrangement can provide an acceptable indoor thermal environment (Figure 9).

These predictions show that in order to make full use of a heat-pipe heat recovery system it is important to control air flow rate. A damper, for example, can be used for this purpose to vary the size of inlet and/or outlet openings. For given air

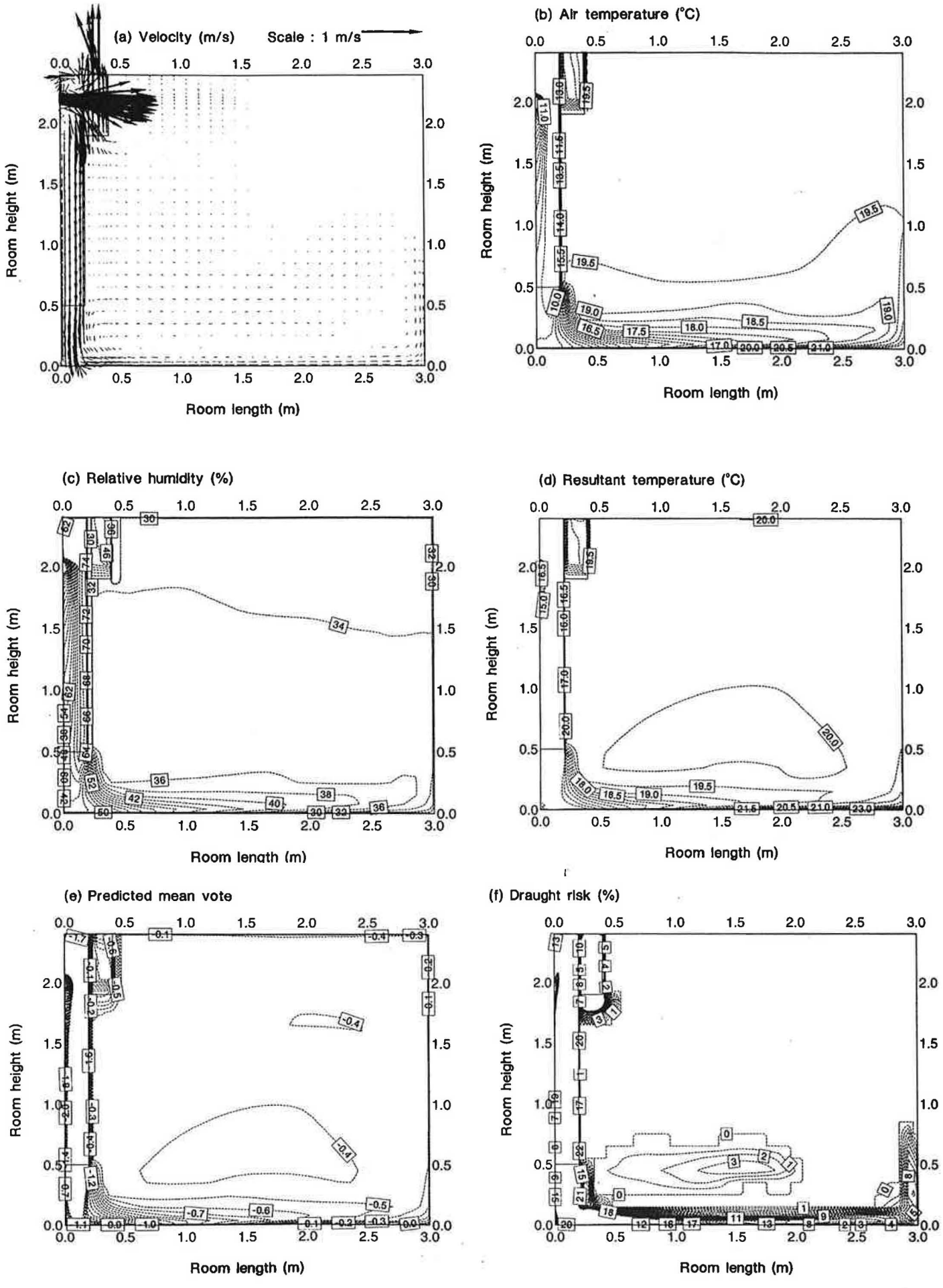

Figure 3 Predicted thermal environment in the room with heat recovery (No. I)

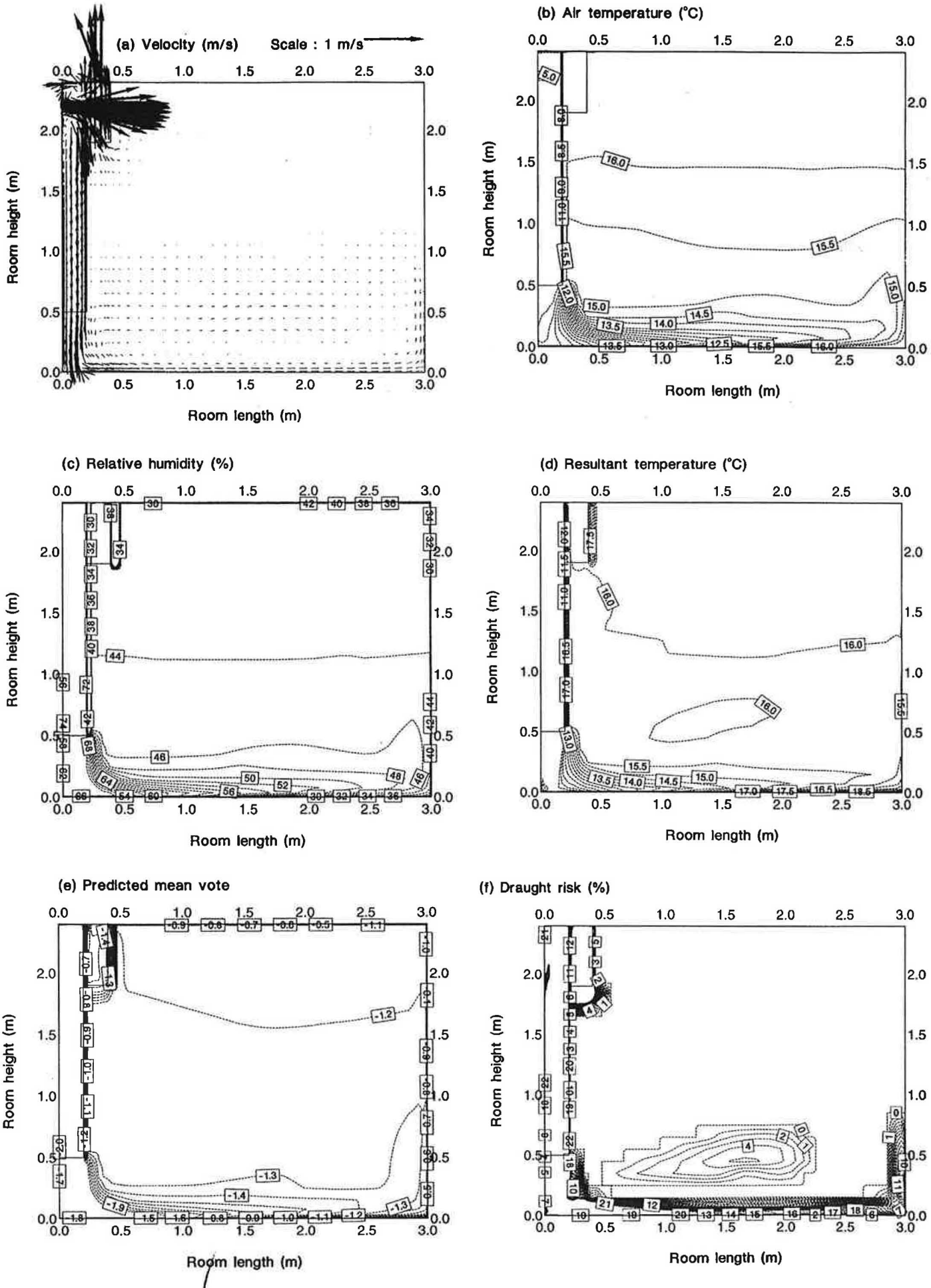

Figure 4 Predicted thermal environment in the room without heat recovery (No. II)

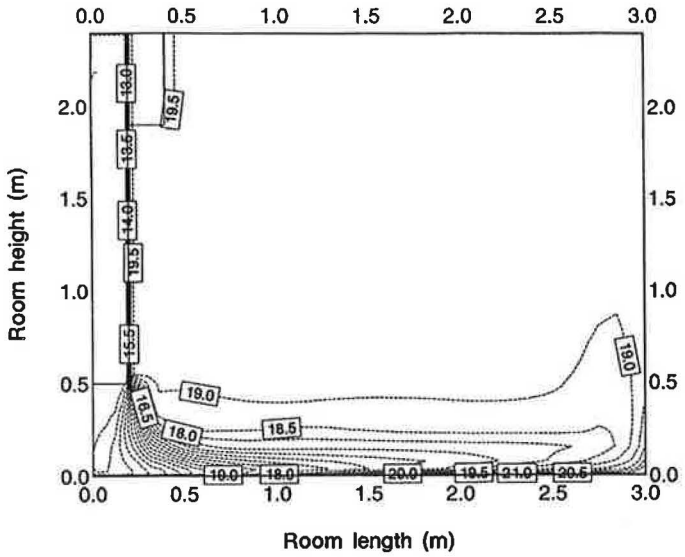

Figure 5 Predicted air temperature (°C) in the room without heat recovery but with increased supply air temperature (10°C) (No. III)

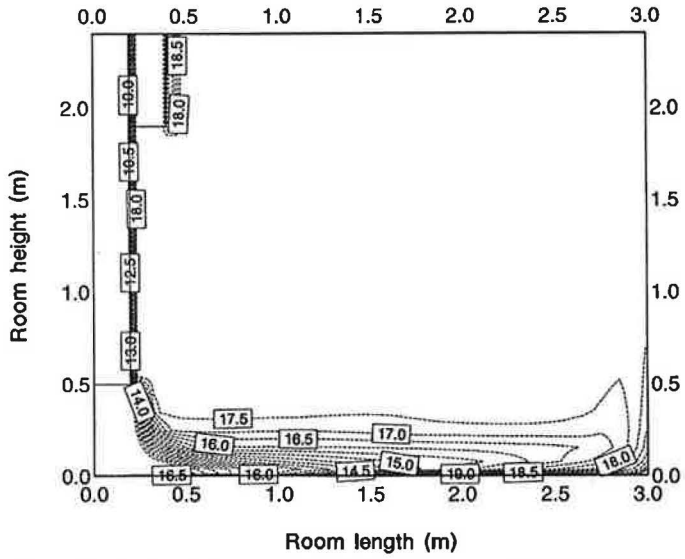

Figure 6 Predicted air temperature (°C) in the room without heat recovery but with increased heat production rate (300 W) (No. IV)

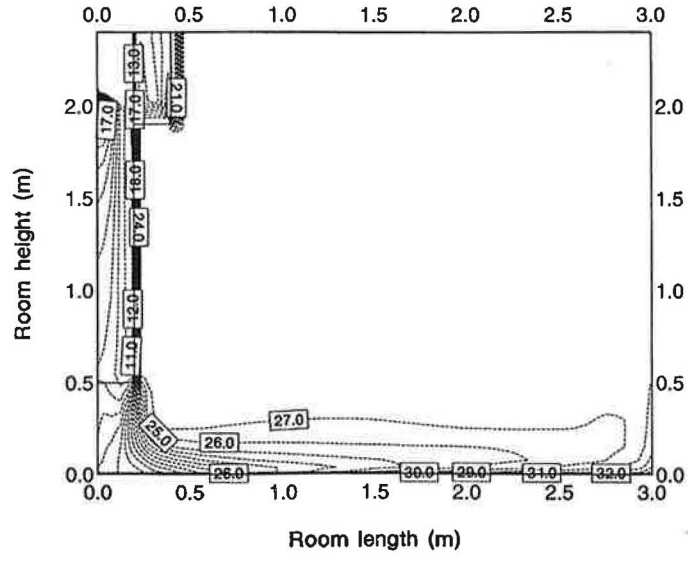

Figure 7 Predicted air temperature (°C) in the room with heat recovery but without wind effect (No. V)

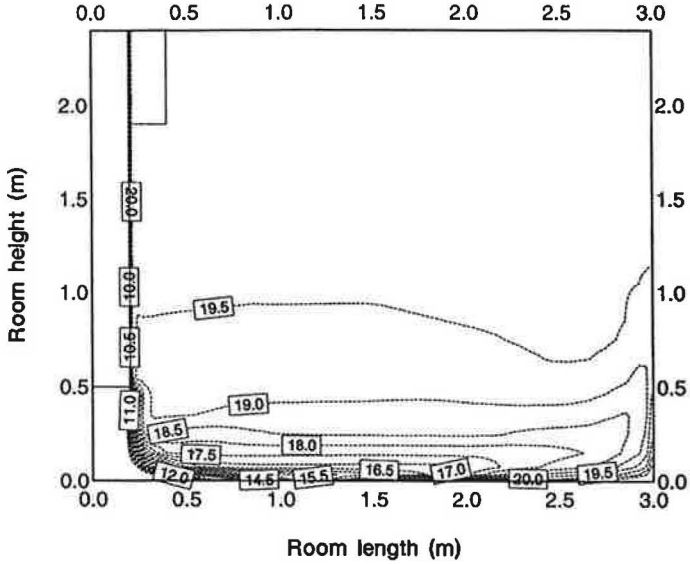

Figure 8 Predicted air temperature (°C) in the room without heat recovery and wind effect (No. VI)

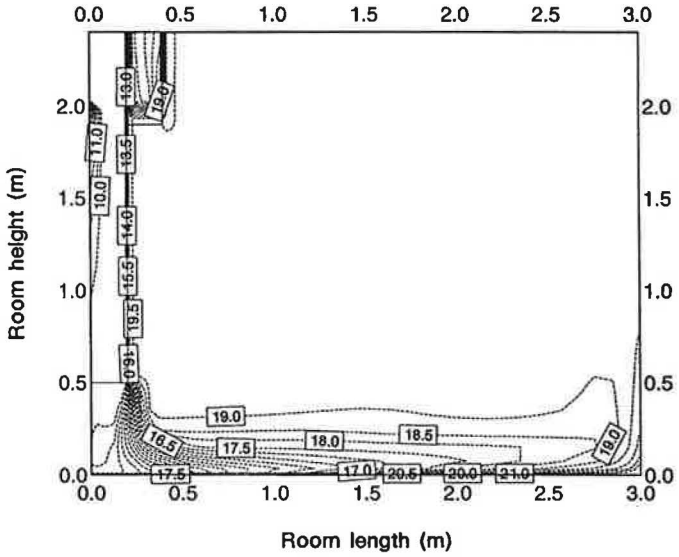

Figure 9 Predicted air temperature (°C) in the room with heat recovery for increased opening size but without wind effect (No. VII)

flow rates, the supply air temperature leaving such a heat recovery system should be regulated in order to prevent more heat recovery than is desired, as shown by No. V. This can be achieved by installing a bypass damper or by changing the orientation of heat pipes.

7 Concluding remarks

Numerical simulations have demonstrated that a heat-pipe heat recovery system can produce adequate thermal comfort with minimum energy consumption in naturally ventilated buildings. To achieve indoor thermal comfort it is essential to control flow rate properly.

The simulations are, however, based on a fixed amount of heat recovery by the heat-pipe unit. In real situations, the efficiency and quantity of heat recovery vary with air flow rate through the unit and the temperatures of supply and return air, as well as the design and arrangement of heat pipes. The influence of these parameters will be investigated in the next stage of research.

Acknowledgement

This project is funded by the Commission of the European Union for JOULE III.

References

1 Dunn P D and Reay D A *Heat Pipes* 4th edn (Oxford: Pergamon) (1994)

2 Hill J M and Lau A S Performance of supermarket air–conditioning systems equipped with heat pipe heat exchangers *ASHRAE Trans.* **99**(1) 1315–1330 (1993)

3 Hill J M and Jeter S M Use of heat pipe heat exchangers for enhanced dehumidification *ASHRAE Trans.* **100**(1) 91–102 (1994)

4 Launder B E and Spalding D B The numerical computation of turbulent flows *Computer Methods in Applied Mechanics and Engineering* **3**(1) 269–289 (1974)

5 Chen Q Comparison of different k–e models for indoor air flow computations *Numerical Heat Transfer, Part B — Fundamentals* 28(3) 353–369 (1995)

6 *CIBSE Guide* Volume A (London: Chartered Institution of Building Services Engineers) (1986)

7 Gan G Numerical method for a full assessment of indoor thermal comfort *Indoor Air* 4(3) 154–168 (1994)

8 Andersen K T Theoretical considerations on natural ventilation by thermal buoyancy *ASHRAE Trans.* **101**(2) 1103–1117 (1995)

9 Gan G and Riffat S B *k*–factors for hvac ducts: Numerical and experimental determination *Building Serv. Eng. Res. Technol.* **16**(3) 133–139 (1995)

10 Gan G and Riffat S B Pressure loss characteristics of orifice and perforated plates *Experimental Thermal and Fluid Science* **14**(2) 160–165 (1997)

11 Yakhot V and Orszag S A Renormalisation group analysis of turbulence *J. Scientific Computing* **1**(1) 3–51 (1986)

12 Yakhot V, Orszag S, Thangam S, Gatski T B and Speziale C G Development of turbulence models for shear flows by a double expansion technique *Physics of Fluids Part A* 4(7) 1510–1520 (1992)

13 Patankar S V *Numerical Heat Transfer and Fluid Flow* (Washington: Hemisphere) (1980)

14 Huang P G and Leschziner M A *An introduction and guide to the computer code TEAM* Report **TFD/83/9** (Manchester, UK: UMIST Dept of Mechanical Engineering) (1983)

15 Fanger P O *Thermal Comfort — Analysis and Applications in Environmental Engineering* (Florida: Krieger) (1982)

16 Fanger P O, Melikov A K, Hanzawa H and Ring J Air turbulence and sensation of draught *Energy and Buildings* **12**(1) 21–39 (1988)

17 ISO 7730: Moderate thermal environments — determination of PMV and PPD indices and specifications of the conditions for thermal comfort (Geneva: International Standards Organisation) (1984)